Review Article

H. Bernhard Schlegel*

Exploring potential energy surfaces

https://doi.org/10.1515/pac-2025-0486
Received April 19, 2025; accepted May 22, 2025

Abstract: Quantum mechanics is central to our understanding of chemistry both qualitatively and quantitatively. Modern electronic structure calculations can yield energies and structures of small to medium size molecules to chemical accuracy, thereby providing a computational model for chemistry. A potential energy surface describes the energy of a molecule as a function of its geometric parameters. The features of potential energy surfaces provide the connections between quantum mechanics and the traditional chemical concepts such as structure, bonding and reactivity. This brief perspective presents an overview of tools for exploring potential energy surfaces such as optimizing equilibrium geometries, finding transition states, following reaction paths and simulating molecular dynamics.

Keywords: Geometry optimization; molecular dynamics; potential energy surface; quantum chemistry; quantum science and technology; reaction path; transition state.

A century ago, a paradigm shift in physics initiated the era of quantum science. Many disciplines have benefited from quantum theory, perhaps none more than chemistry (see quote by Dirac[1]). In the past 100 years, quantum mechanics has grown from a novel mathematical theory of interest primarily to physicists to a practical everyday world view for chemists. Quantum theory is vital for the description of electrons and hence the behavior of molecules and ultimately the understanding of chemistry. Through advances in theoretical approaches, numerical methodology, user-friendly software and especially computational resources, quantum chemistry has joined the mainstream of research in chemistry and related disciplines. The intent of this short perspective is to look at potential energy surfaces as the link between the quantum nature of the electronic structure of molecules and traditional chemical concepts such as molecular structure, reactivity, dynamics and reaction mechanisms.

The experimental study of the structure and energetics of molecules has a long history. However, most of the experimental methods are limited to molecules close to their equilibrium geometry. These methods give us snapshots of molecules rather than movies of molecules undergoing reactions. By contrast, modern quantum mechanical methods can calculate a molecule in any geometry. Methods such as density functional theory[2–4] can reliably model the behavior of molecules and materials with hundreds to thousands of atoms. For small to medium size molecules quantum chemistry can calculate energies, structures and properties to near chemical accuracy by using various compound and extrapolation methods (see ref. 5 and references therein). In essence, quantum theory provides us with a model chemistry (see Pople's Nobel lecture[6]) that we can use to explore the actions of molecules in ways that are not readily accessible by experimental methods. Several of the articles in this issue demonstrate the power of computational methods based on quantum theory in exploring a variety of topics in chemistry.

Potential energy surfaces are central to the application of quantum theory to chemistry. A potential energy surface describes the energy of a molecular system as a function of the coordinates of the atoms that make up the

Article note: A collection of invited papers to celebrate the UN's proclamation of 2025 as the International Year of Quantum Science and Technology.

***Corresponding author: H. Bernhard Schlegel**, Department of Chemistry, Wayne State University, Detroit, MI 48202, USA, e-mail: hbs@chem.wayne.edu. https://orcid.org/0000-0001-7114-2821

system.[7] Figure 1 shows a model potential energy surface with some of its features.[8] In this simple three-dimensional model, the energy is plotted vertically, and two geometric coordinates are plotted horizontally. Polyatomic molecular systems have many more than two geometric coordinates. However, two coordinates are sufficient to illustrate the key features of potential energy surfaces.

It is helpful to think of a potential energy surface as a hilly landscape and this analogy is used to describe the features illustrated in Fig. 1. The valleys in this landscape are related to molecules. In particular, the geometric coordinates of the bottom of a valley correspond to the equilibrium structure of a molecule. Movements close to the bottom of the valley describe molecular vibrations. An elementary reaction corresponds to traveling from the valley for the reactants to a neighboring valley for the products. The difference in the heights of the valley floors is the reaction energy, and the height of the mountain pass between the valleys is the barrier for this elementary reaction. The lowest energy route from reactants to products is the reaction path. The highest point along the lowest energy reaction path is the transition structure (TS) for the reaction. The steepest-descent path in mass-weighted coordinates down from the TS to the reactants and products is termed the intrinsic reaction coordinate (IRC).[9] The tangent to the IRC at the TS is the transition vector. In some cases, the reaction path can descent from a transition structure and branch into two different valleys. A valley-ridge inflection (VRI) point is where the curvature perpendicular to the path changes from positive to negative and is associated with branching on symmetric surfaces. The TS is a first order saddle point on the Born-Oppenheimer surface with maximum in one and only one direction, and a minimum in all other directions. Transition structure and transition state are often used interchangeably, but technically the latter would include zero-point vibration and thermal corrections for the highest energy point on the reaction path. Figure 1 also shows a number of second order saddle points. These are maxima in two directions and minima in all other directions. If there is a second or higher order saddle point along the ridge separating reactants and products, there is always a lower energy transition structure and reaction path. Since the forces on the atoms are zero at minima, first order saddle points and higher order saddle points, they are also known as stationary points.

The concept of a potential energy surface is the result of the Born-Oppenheimer approximation.[10] In solving the Schrödinger equation, this approximation assumes that the wavefunction for the electrons and the nuclei can be treated separately. In particular, the electronic wavefunction and energy can be calculated as a function of the positions of stationary nuclei. Using the lowest energy wavefunction, the Born-Oppenheimer approximation yields a potential energy surface for the ground state. Higher energy solutions of the Schrödinger equation produce potential energy surfaces for excited states. The Born-Oppenheimer approximation is good if these surfaces remain well separated but breaks down if the surfaces get too close, touch or intersect. In such cases, the quantum behavior of electrons and nuclei must be treated together without invoking the Born-Oppenheimer approximation.

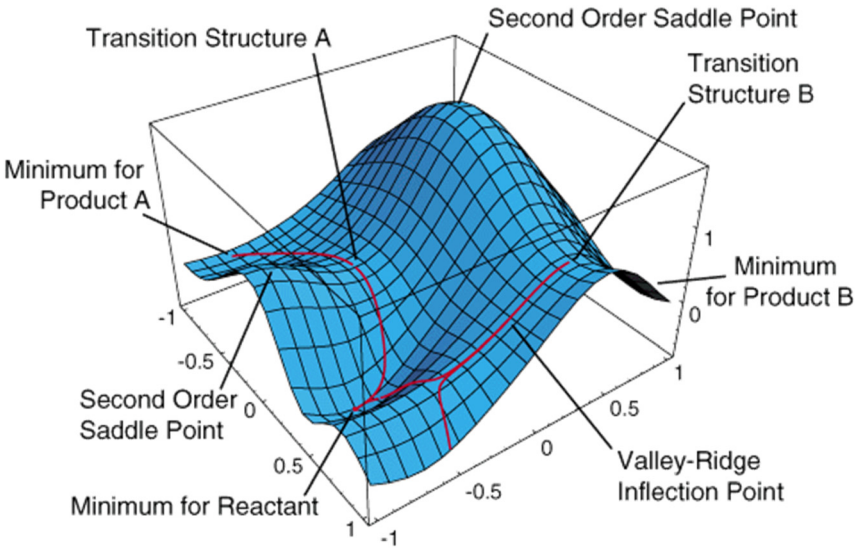

Fig. 1: Model potential energy surface showing minima, transition structures, second order saddle points, reaction paths and a valley ridge inflection point (reprinted with permission from ref. 8. Copyright 2011 John Wiley & Sons).

A potential energy surface can be constructed by calculating the energy for many different geometries and fitting a functional form to the data.[11–18] This is a costly and tedious process that is suitable only for small systems. Numerous potential energy surfaces have been developed for gas-phase reactions since the 1970s.[19] In recent years, potential energy surfaces have been constructed with machine learning in the form of neural networks.[20–23] This approach has largely replaced fitting potential energy surfaces with an explicit functional forms. Needless to say, constructing full potential energy surfaces is a costly way to find minima, transition states and reaction path. If derivatives of the potential energy with respect to geometric parameters are available, these features can be located directly without explicitly constructing a potential energy surface.

While total energies have been a goal of quantum calculations from the beginning, efficient analytic methods for calculating first derivatives of the energy with respect to geometric parameters (also known as force or gradients) were not developed until the late 1960s. One of the landmarks is Pulay's 1969 paper[24] for practical first derivatives of the Hartree–Fock energy with respect to geometrical parameters (*i.e.* forces on the atoms). Instead of using the Hellmann-Feynman theorem, Pulay's method involves derivatives of all of the integrals, including the two-electron Coulomb and exchange integrals. For Hartree–Fock (HF) and density functional theory (DFT), the first derivatives with respect to geometric parameters or gradients can be calculated in about the same time as the energy, giving the forces on all of the atoms in the molecular system. As new, more accurate levels of theory that included electron correlation have been developed, analytic energy derivative methods followed within a few years (see refs. 25–31 for examples).

The implementation of analytic first derivatives was soon followed by the development of practical methods for analytic second derivatives (also called the Hessian or force constant matrix).[30,31] Analytic second derivatives of the Hartree–Fock energy[25] cost about N times that of the gradients for an N atom system. Analytic Hessians are also available for a number of higher levels of wavefunction theory that include electron correlation.[32–36] Together with energy derivatives with respect to the electric field, these calculations provide a straight-forward way to calculate harmonic vibrational spectra and infrared and Raman intensities at an affordable cost.[30,31] Analytic third and fourth derivatives are also available for some levels of theory.[30,31,37]

Exploring potential energy surfaces includes finding equilibrium geometries, calculating relative energies, locating transition structures and following reaction paths to map out reaction mechanisms.[7] With the aid of energy derivatives these tasks can be carried out directly without needing to fit a potential energy surface. Calculating an equilibrium geometry corresponds to finding a point on the potential energy surface that is a minimum. This can be achieved by using the first derivative to follow the surface downhill until all of the forces on the atoms are zero and the curvature in all directions is positive. Locating a transition structure is not as easy, since this requires a stationary point on the potential energy surface that is a maximum in one direction and a minimum in all other directions. Part of the difficulty is that the direction for maximization is not known in advance and that the region around transition states that has the correct curvature (*i.e.* maximum in one and only one direction) is much smaller than around minima. Specialized algorithms have been developed for transition structure optimization and are discussed below. Once a putative transition structure has been found, it must be checked using a second derivative or vibrational frequency calculation to make sure that it has one and only one negative eigenvalue or imaginary vibrational frequency. It is also necessary to confirm that the transition structure is appropriate for the reaction of interest by checking the transition vector or by following the reaction path downhill to the reactants and products. This brief perspective highlights some of the successful approaches to exploring potential energy surfaces. Details of numerical methods and associated equations for exploring potential energy surfaces can be found in a number of reviews and original papers cited therein.[7,8,38–40]

Exploring a potential energy surface requires a choice of coordinates to represent the structure of the molecule. Cartesian coordinates are the simplest and most general. Electronic structure codes use Cartesian coordinates to compute the necessary integrals and calculate the wavefunctions, energies, derivatives and properties. Cartesian coordinates and fractional coordinates in a unit cell are quite suitable for the geometries of surfaces and solids. By contrast, Cartesian coordinates are a poor choice for molecules. Internal coordinates such as bond lengths, valence angles and dihedral angles[41–43] are better for molecules since they reflect the structure and bonding of a molecule and are not affected by the overall translation and rotation of the molecule. The number of internal coordinates need for a molecule with N atoms is 3 N – 6 (or 3 N – 5 if it is linear). However,

molecules often have more than 3 N – 6 internal coordinates, especially for cyclic systems. The conversion of these redundant internal coordinates to Cartesian coordinates for electronic structure calculations involves a generalized inverse or singular value decomposition to remove the degrees of freedom that cannot be represented in Cartesian coordinates. Primitive redundant coordinates involve all bond lengths, valence angles and dihedral angles.[41,43] Natural internal coordinates employ coordinates used to describe vibrational motions, such as rock, umbrella bend, ring breathing etc.[41,42] Generalized internal coordinates allow for linear combinations and various functions of coordinates and may be helpful for highly symmetrical molecules.[44] The choice of a good coordinates system can significantly accelerate tasks such as geometry optimization by reducing the coupling between coordinates.

One of the first tasks in exploring potential energy surfaces is to find the minima that represent the equilibrium structures relevant to the system under investigation. The closest local minimum can be found by following the potential energy surface downhill. This is relatively easy using analytic first derivatives. By contrast, finding the global minimum of a potential energy surface can be a very difficult problem. Some rigorous and deterministic algorithms are available, but a general discussion of global optimization[7] is beyond the scope of this brief perspective.

Conjugate gradient algorithms are some of the older methods for minimization and require relatively little memory.[45,46] Given a search direction, a minimum is found by a line search using just the energy. The gradient is calculated at the minimum of the line search. Using the gradient, the next search is in a conjugate direction (rather than in a perpendicular direction) in order to maintain the minimum in the previous search direction. This is repeated until the gradient is below a threshold.

If the Hessian or second derivatives are available, the potentials energy surface can be modelled locally by a quadratic expression. In the local quadratic approximation, the energy is $E(\Delta\mathbf{x}) = E_0 + \mathbf{g}_0^{\mathrm{T}}\Delta\mathbf{x} + 1/2\Delta\mathbf{x}^{\mathrm{T}}\mathbf{H}_0\Delta\mathbf{x}$, in terms of the displacement $\Delta\mathbf{x}$, current energy E_0, gradient $\mathbf{g}_0$ and Hessian $\mathbf{H}_0$. The corresponding gradient is given by $\mathbf{g}(\Delta\mathbf{x}) = \mathbf{g}_0 + \mathbf{H}_0\Delta\mathbf{x}$. Setting the gradient to zero and solving for the displacement $\Delta\mathbf{x} = -\mathbf{H}_0^{-1}\Delta\mathbf{x}$ yields the minimum on this local quadratic surface. This is called a Newton or Newton Raphson step.[47,48] Because actual potential surfaces are not quadratic, this may need to be repeated several times to reach the minimum.

Second derivatives are more costly to calculate than first derivatives (up to N times, where N is the number of degrees of freedom). By starting with an approximate second derivative matrix or Hessian, an updating method can be used to improve the approximate Hessian during the course of the optimization. This is the quasi-Newton method for optimization.[47,48] Some of the updating methods are SR1, BFGS and BSP, and they are chosen so that updated Hessian fits the gradient at the current and previous step. For minimization, the update should be positive definite and symmetric; BFGS[49–52] is one of the best. Similar formulas are available for updating the inverse of the Hessian, thereby avoiding the need for a matrix inverse at each step. A line search is not necessary for quasi-Newton methods so long as the step satisfies the Wolfe conditions[53] for reducing the function value and magnitude of the gradient. For very large dimensional systems, storage of the Hessian may be a problem. The L-BFGS algorithm,[54] the limited memory version of BFGS, avoids storage of the full Hessian by starting with a diagonal inverse Hessian and updating it using a fixed number of recent optimization steps.

Another effective approach for geometry optimization is the direct inversion of the iterative subspace (GDIIS),[55,56] An error matrix is constructed for each linearly independent step of the optimization using the energies and gradients of the current and previous points. A linear combination of the previous steps is chosen to minimize the error and provide the best step to the next point in the optimization. As in the quasi-Newton method the Hessian is updated each step. Going beyond the quadratic model that is the basis of quasi-Newton methods, machine learning methods such as Gaussian process regression, gradient-enhanced Kriging and Bayesian methods have also been used for geometry optimization.[57–60]

The Newton, quasi-Newton and GDIIS methods are based on a local quadratic approximation to the potential energy surface. If any of the eigenvalues of the Hessian are too small, these methods can step beyond the quadratic region or even in the wrong direction if any of the eigenvalues are negative. One approach for controlling the step size is the trust radius method.[47,48] If a step is larger than the current trust radius, the step size is reduced by scaling the step or by finding the minimum energy for a step with the current trust radius. The energy and gradient are used to update trust radius so that it is a good estimate for the size of the quadratic region

around the current point. Rational function optimization[61–63] (RFO) is an alternate approach for controlling the step size and direction. The energy is written as a quadratic function divided by another quadratic function, with the latter used to scale the step. Minimizing the energy of the RFO expression leads to a step of $\Delta x = -(\mathbf{H}_0 - \lambda\mathbf{I})^{-1}\,\mathbf{g}_0$. For minimization, the constant λ is chosen so that $(\mathbf{H}_0 - \lambda\mathbf{I})$ has no negative eigenvalues and yields a step of the desired length.

The algorithms for finding minimum energy geometries are very robust. This has led to very large data sets with up to 100,000,000 optimized molecular structures (OMol25,[64] ANI-1[65,66] and PubChemQC[67]). These can be used for benchmark studies of new electronic structure and density functional methods, and for training machine learning and artificial intelligence. By using the energies at equilibrium geometries and systematic displacements along vibrational modes, these data sets have also been used to train neural networks to reproduce energies and optimized structures.[64–66,68] The results are better than semi-empirical quantum methods and rival ab initio and density functional quantum methods for molecules within the scope of the training set.

Finding transition structures (TS) is more difficult than optimizing equilibrium structures because the direction for maximization is often not known in advance and because the quadratic region around the TS that has the correct curvature (*i.e.* a maximum in only one direction) is much smaller than region where optimization lead to minimum. If the initial guess for the TS geometry is within the quadratic region (*i.e.* where the Hessian has only one negative eigenvalue) and the full Hessian has been calculated, then the TS can be found using a series of Newton steps with suitable step size control. Minimizing the norm of the gradient is an alternative,[69] but the quadratic region for the gradient norm is even smaller and some of the minima of the gradient norm are inflection points rather than TS's. More often than not, it is difficult to obtain a good start structure for a TS optimization. The key task of most TS searching methods is to get close enough to the TS so that quasi-Newton methods can be used to optimize the TS. These can be classified into double-end methods that use structures in the reactant and product valleys to bracket and localize the TS and single-ended methods that start in one valley and climb toward the TS.[7]

Examples of single-ended strategies for getting close to the transition state include walking up valleys, coordinate driving, Newton trajectories, reduced gradient following, gradient extremals and artificial force induced reaction methods. Walking up the shallowest ascent[70] can be accomplished in a number of ways. Quasi-Newton approaches based on Lagrangian multipliers, RFO or partitioned RFO[61–63,70–72] are similar methods for walking up valleys, and each uses a step of the general form $\Delta x = -(\mathbf{H}_0 - \boldsymbol{\lambda})^1\,\mathbf{g}_0$ with the λ's chosen so that $(\mathbf{H}_0 - \boldsymbol{\lambda})$ has one negative eigenvalue and the step has the desired direction and length. Gentlest ascent dynamics[73] is the trajectory version of walking up valleys to transition states, analogous to steepest descent dynamics for finding minima. In the dimer method,[74–76] two test structures are separated by a short, fixed distance and this dimer is rotated to find the lowest energy. In this orientation, the dimer points along the valley floor and can be moved uphill toward the TS. However, these methods may not lead to the desired transition state if the reaction path is not along the shallowest valley. Coordinate driving is an alternative:[77,78] a step is taken toward the TS along the chosen coordinate and the energy is minimized with respect to the remaining coordinates; the chosen coordinate is incremented and the process is repeated. Newton trajectory and reduced gradient following methods[79–82] are closely related to coordinate driving: a gradient direction is chosen and the energy is minimized perpendicular to this direction; a step is taken uphill toward the TS and the process is repeated. These can work well if a single coordinate or direction dominates the reaction path but can fail if the path is strongly curved and the direction changes as the TS is approached. Another method is to follow a gradient extremal path,[83–86] defined as the path for which the gradient is an eigenvector of the Hessian. Gradient extremals pass through TS's and minima; however, they tend to wander about the potential energy surface making them less practical. For bimolecular systems, the artificial force induced reaction[39] (AFIR) method works by applying a force to pull reactants together until the TS is reached.

One of the simplest double-ended approaches is to start with a structure in the reactant valley and a structure in the product valley and search for a maximum along a linear or quadratic path connecting these structures, *e.g.* linear synchronous transit, LST, or quadratic synchronous transit,[87] QST. In the QST2/QST3 method,[88] a maximum is found along a path in redundant internal coordinates and then the TS is fully optimized using Newton or quasi-Newton methods (QST3 adds a third structure to provide a guess for the TS and the curvature of the path). The

Hessian updating method for TS optimization must be able to maintain a negative eigenvalue. BFGS is not suitable, but Bofill has devised a combination of SR1 and PSB Hessian updates that works well.[89] It is beneficial to use a smaller trust radius than for minimization. The RFO method provides a good way to control the step size and direction.[61–63] The constant λ in the RFO step $\Delta x = -(\mathbf{H}_0 - \lambda\mathbf{I})^{-1}\,\mathbf{g}_0$ needs to be chosen so that $(\mathbf{H}_0 - \lambda\mathbf{I})$ has one and only one negative eigenvalue and the step length equal to or smaller than the trust radius. This can be applied to the full Hessian or the Hessian can be partitioned into one or a few eigenvectors that dominate the TS and the remainder for minimization.[61–63,90,91]

The double-ended chain-of-states approaches such as nudged elastic band[92–95] (NEB) and string methods[96–100] (SM) are more robust than single-ended walking up valleys and coordinate driving methods. The calculation starts with a series of equally spaced structures along an initial estimate of the path connecting reactants and products. For NEB, spring forces are added between the structures to keep them equally spaced (sometimes additional springs are needed to keep the path from bending too sharply). For string methods, reparameterization of the positions maintains equal spacing between the structures. The forces perpendicular to the path are minimized to relax the structures toward the minimum energy path. This is illustrated in Fig. 2. The structures closest to the TS can then be fully optimized using a Newton or quasi-Newton method. These approaches are also suitable for reaction paths with multiple transition states and intermediates. Numerous energy and gradient calculations may be needed for each of the points along the path because their optimizations are strongly coupled. Constrained quasi-Newton optimization and Gaussian process regression are alternative approaches for relaxing the structures toward the reaction path.[101–103] Growing string (GSM) and freezing string (FSM) methods[99,100] reduce the amount of computation by starting with the two end structures of the path and adding and optimizing one structures at a time to build up the full path and reach the TS.

Once a TS has been optimized, a second derivative calculation or frequency calculation is required to confirm that it is indeed a transition state with only one negative eigenvalue or imaginary frequency. The transition vector is the normal mode with the imaginary frequency and should correspond to motion between the desired reactants and products. Often it is also necessary to follow the steepest descent path from the TS to the reactants and to the products to be sure that it is the correct TS for the intended reaction. A steepest descent path or minimum energy path in mass-weighted coordinates is the intrinsic reaction coordinate (IRC).[9]

A steepest descent path or minimum energy path is defined such that the gradient is tangent to the path at every point. In principle, the reaction path can be found by starting at the TS and stepping downhill in the direction of forces on the atoms. However, very small steps are needed to prevent the path from zigzagging as it

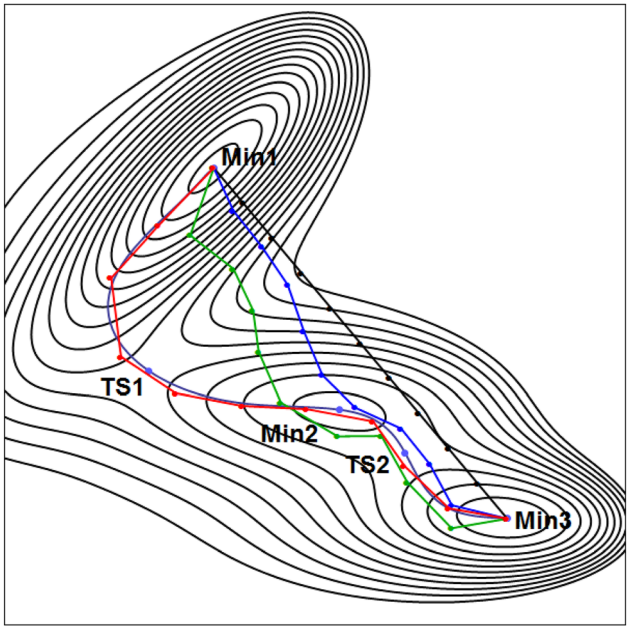

Fig. 2: An example of a double-ended reaction path optimization on the Muller-Brown surface. The path optimization with 11 points starts with the linear synchronous transit path (black); the few intermediate iterations of the path optimization are shown in blue and green. The final path in red can be compared with the steepest descent path in light blue (reprinted with permission from ref. 8. Copyright 2011 John Wiley & Sons).

descends the valley. Several methods have been developed to follow the reaction path accurately and efficiently with larger step sizes.[104–113] In particular, implicit methods for differential equations and predictor-corrector methods with updated Hessians are efficient and stable methods following the path.[109–113] Approximate reaction paths can also be obtained from chain-of-states approaches such as NEB[92–95] and string methods.[96–100] In addition to connecting the TS to reactants and products, a steepest descent path can be used to construct a reaction path Hamiltonian to to investigate aspects reaction dynamics.[114,115] The reaction path can also be used to obtain information about the sequence of different elements of a reaction (such as bond making/breaking, conformational changes, electronic reorganization) using the unified reaction valley analysis[115–117] (URVA) approach.

In some cases, the valley descending from a TS toward products can bifurcate yielding two different products from a single transition state. Recently there has been considerable experimental interest in bifurcating or ambimodal reactions (for some recent examples, see refs. 118–131) For a symmetric potential energy surface, bifurcation is characterized by a valley-ridge inflection (VRI) point (see Fig. 1). These can be found by following the IRC and monitoring the second derivatives perpendicular to the reaction path. The VRI point is where the lowest eigenvalue of the second derivatives perpendicular to the steepest descent path changes from positive (valley) to negative (ridge).[132,133] For a more general case of bifurcation on an asymmetric potential, the IRC does not pass through a VRI point and stay on the ridge, but descends into one of the two valleys.[118,119] The branching ratio between the two valleys can be found by classical trajectory calculations on the surface.[134] Methods that systematically explore potential energy surfaces can also locate bifurcations of valleys and characterize ambimodal reactions.[133,135,136] Approximate methods have also been devised to estimate the branching ratio.[126,127]

A reaction mechanism on ground state potential energy surfaces may consist of multiple elementary steps, various intermediates and numerous transition structures. For a complicated reaction, this may be intractable to carry out manually. Automated workflows are being developed to explore reaction networks (for some reviews see refs. 40, 137, 138). Some of the interesting methods are briefly summarized here. Maeda and co-workers[39] have automated the use of AFIR and ADDF (anharmonic downward distortion following) to map multistep reactions and to find all of the transition structures and intermediates. Zimmerman and co-workers[40] have developed *ZStruct* to explore the reaction space of molecular systems. Connectivity graphs are used to determine potential intermediates and the growing string method (GSM) is used to find the connecting transition states. Habershon[139,140] has developed an automated approach for finding reaction mechanisms using connectivity-based sampling, NEB for exploring potential energy surfaces and kinetic simulations of reaction networks. The Reaction Mechanism Generator (RMG) of Green et al.[141] constructs kinetic models using thermochemistry and estimated rates from a database of reaction templates. Subsequently, they used automated energy surface exploration to generate 12,000 organic reactions involving H, C, N and O.[142] In the "nanoreactor" approach developed by Martinez and coworkers,[143] a mixture of reactants is place in a container and lengthy molecular dynamics runs at high temperature and high pressure are used to see what reactions occur. Successful chemical transformations then are refined to obtain intermediates and transition states. *Crystal*, the software package developed by Poirier and co-workers,[136] systematically traverses the potential energy surface for selected degrees of freedom using a grid-based search strategy. The grid is expanded in a series of increments until a maximum energy is reached and all of the relevant features of the potential energy surface have been located. Reiher and coworkers[136] have developed the *Chemotron* software package to explore reaction networks. Based on first principles heuristic rules derived from electronic wavefunctions, reactive sites are detected, reaction networks are generated and elementary reactions in the network are refined by quantum chemical methods. Meuwly[144] has reviewed machine learning for chemical reactions, including rates and reaction networks. Clearly, this is a hot area and more progress can be expected in coming years.

Photochemical reactions involve potential energy surfaces for excited states and transition rates between them. Transitions between surfaces are most probable near seams of intersection and conical intersections.[145,146] Surfaces for states of different spin or spatial symmetry can cross at seams of intersection. For a surface with N degrees of freedom, the seam has N–1 degrees of freedom and transitions between the surfaces are most probable near the minimum energy point along the N–1 dimensional seam of intersection. States with the same spin and spatial symmetry can interact resulting in an avoided crossing rather than a seam of intersection. However, the surfaces can intersect where the interaction matrix element goes to zero, forming a seam with N–2 degrees of

freedom. The lowest point on this N–2 dimensional seam is the minimum energy conical intersection. Figure 3 shows the potential energy surfaces for the ground state and first excited state of C_2H_4 and the conical intersection connecting these two surfaces. To properly locate conical intersections, the two energy surfaces must be calculated with comparably accurate electronic structure methods.[147] This usually requires complete active space self-consistent field (CASSCF) calculations, complete active space second order perturbation theory (CASPT2) or multi-reference configuration interaction (MRCI). Optimizing the structure of a minimum energy seam crossing or conical intersection involves moving across the potential energy surfaces to reach the seam where the two surfaces have the same energy and then following the N–1 or N–2 dimensional seam to find the minimum. A number of algorithms have been developed to find minimum energy seam crossing and conical intersections.[147–162] The penalty function method[149,150] minimizes the average of the two energies $(E_I + E_J)/2$ plus a function of the difference in the energy of the surfaces, $\Delta E_{IJ} = E_I - E_J$. In the projection approach,[151–154] the gradients of ΔE_{IJ} and H_{IJ} (the interaction matrix element between the surfaces) are used to define a 2 dimensional space where the square of the energy difference is minimized. In the remaining N–2 dimensional space, the energy of the upper surface is minimized. In the Lagrangian multiplier method,[155–161] $L = E_I + \lambda_1 \Delta E_{IJ} + \lambda_2 H_{IJ}$ is minimized with respect to the geometry and the Lagrangian multipliers λ_1 and λ_2. Algorithms have also been developed to follow seams of intersection.[151] Similar to finding all of the minima and transition states for a reaction mechanism, it can be challenging to finding all of the relevant conical intersection for a photochemical process. Maeda and coworkers have adapted the AFIR method to automatically find all of the conical intersections between two states.[154] The *Crystal* program has been enhanced to systematically search for the conical intersection between multiple surfaces.[162] The nanoreactor approach of Martinez and co-workers has been extended to non-adiabatic reactions and locates all of the relevant conical intersections.[163]

Molecular motions during reactions explore larger regions of potential energy surfaces than just stationary points and steepest descent paths. While electron dynamics must be treated by quantum mechanics, molecular dynamics can most often be treated by classical mechanics because nuclei are much heavier than electrons. A number of decades ago calculating classical trajectory on potential energy surfaces[165–167] required fitting a functional form to the potential energy surface.[11–18] With the increase in computational power in recent decades, classical trajectories can be calculated directly by using electronic structure methods to compute the forces on the

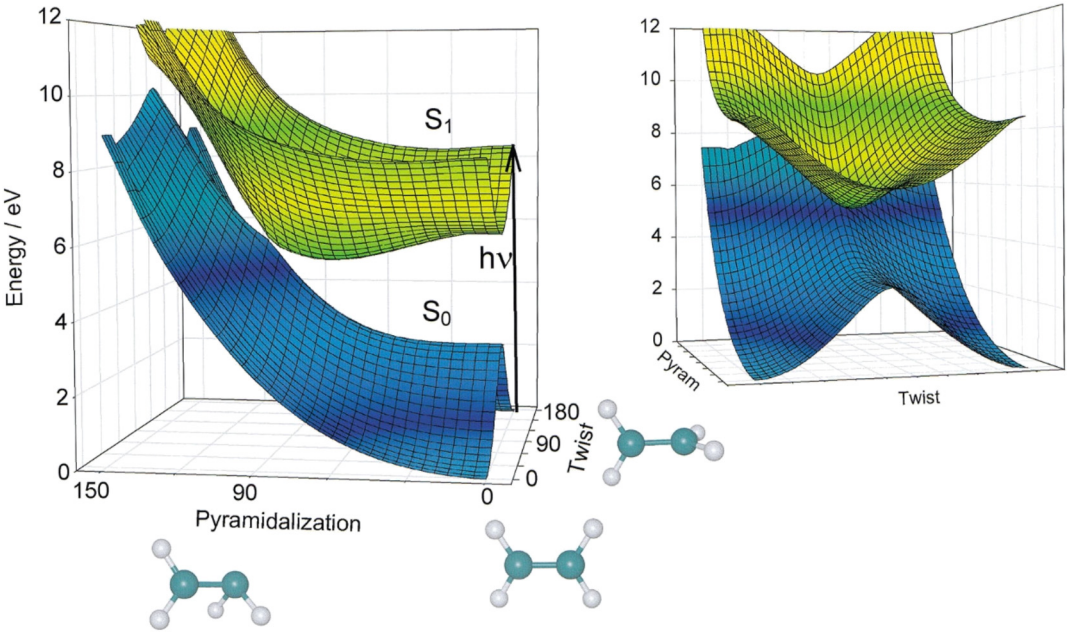

Fig. 3: Two views of the ground and first excited electronic states of C_2H_4 and the conical intersection between these two surfaces (reproduced with permission from ref. 164. Copyright American Chemical Society 2000).

atoms in the molecule on-the-fly, every time they are needed for integrating the classical equations of motion.[168,169] Symplectic integrators such as velocity Verlet[170] and higher order versions[171,172] ensure conservation of energy. If second derivatives are available, Hessian-based predictor corrector algorithms with Hessian updating can be used to take larger steps,[173–175] reducing the number of electronic structure calculations while maintaining good energy conservation. The cost of the electronic structure calculations can be reduced by propagating the wavefunction or the electron density along with propagating the nuclei using an extended Lagrangian.[176] This approach is used in Car-Parrinello dynamics[177–179] (*e.g.* CP2K) for the condensed phase and density matrix propagation[180–182] (ADMP) for molecular systems. To obtain reliable statistics in molecular dynamics studies, hundreds to thousands of trajectories may be needed. The GROW procedure of Collins and coworkers[183] builds up an interpolated potential energy surface from trajectories calculated on-the-fly, thereby reducing the number of electronic structure calculations for the additional trajectories needed to obtain statistically significant results. Highly accurate electronic structure methods may be too costly for on-the-fly direct dynamics. In this case, fitting a functional form to a large number of high-level electronic structure calculations is the preferred approach.[11–18] This is facilitated by the use of permutationally invariant polynomials.[15–17] Increasingly, neural networks are being used to fit a large set of electronic structure calculations to provide a potential energy surface for molecular dynamics calculations.[21,184–186]

Some cases, such as hydrogen atom tunneling through a barrier, require a quantum mechanical treatment of a few atoms in a molecular system. Ring polymer and centroid dynamics[187] can be used to calculate quantum trajectories. These can be calculated on-the-fly using energy and gradients calculated by electronic structure methods at each step in the trajectories.[188–193] Nuclear wavepackets for selected light atoms can be propagated on a local grid that travels with the molecule.[194–198] Alternatively, selected nuclei can be included in the wavefunction in the nuclear-electron orbital (NEO) method[199,200] using Hartree–Fock, density functional and correlated methods to calculate both the nuclear and electronic wavefunctions and their interactions.

The investigation of dynamics of photochemical reactions[147,201–208] is more challenging than ground state thermal reactions. Photochemical dynamics typically involve numerous surfaces and transitions between them. These surfaces and interactions between them are much more difficult to fit than for the ground state where structure, bonding and reactivity are well understood. Thus, computing dynamics directly from electronic structure calculations is even more important for photochemical reactions. This is a rapidly expanding area of method development and several excellent reviews are available.[201–208] Only a very brief overview is provided here. Electronic structure calculations need to be able to represent the relevant excited states on an equal footing. Like searches for conical intersections, this may involve CASSCF, CASPT2, MRCI, equation of motion coupled cluster (EOM-CC) and related methods. On-the-fly classical trajectories provide a description of dynamics on an individual excited state surface. Non-adiabatic transitions to lower energy surfaces can be modelled with fewest switching and related surface hopping methods.[209–211] Ab initio multiple spawning (AIMS) methods[204] represent the nuclear wavefunction by Gaussian wavepackets guided by classical trajectories calculated on-the-fly. The wavepackets can split (spawn) into separate wavepackets at surface crossings and conical intersections. In Ehrenfest dynamics, a Gaussian wavepacket is propagated in the mean field of the electronic states.[209,212] When a decoherence correction is added, Ehrenfest dynamics yields the correct collapse to the final states.[213] Multiconfiguration Ehrenfest (MCE) dynamics[214] propagates a set of interacting wavepackets to obtain correct quantum dynamics and decoherence. In the variational multiconfigurational Gaussian (vMCG) method,[215] the Gaussian wavepackets follow coupled quantum trajectories. There are still many challenges for non-adiabatic dynamics on excited state potential energy surfaces. This will continue to be a very active area of research.

Summary

A potential energy surface represents the energy of a molecule as a function of its geometric parameters. It provides an easily visualized connection between quantum chemical calculations of the electronic structure of a molecule and chemical concepts such as geometry, bonding and reactivity. A potential energy surface can be thought of as a hilly landscape, with valleys corresponding to reactants and products. Connections between

different valleys are reaction paths and transition states are mountain passes along reaction paths. These features can be found directly without constructing a full potential energy surface by using methods that employ energy derivatives. This article provides an overview of tools for exploring potential energy surfaces and briefly discusses methods for optimizing equilibrium geometries, finding transition states, following reaction paths and simulating molecular dynamics. Two active and challenging areas of research in the exploration of potential energy surfaces are the automated workflows for the exploration of reaction networks and the development of methods for non-adiabatic dynamics of photochemical reactions.

Acknowledgments: This work was supported by a grant from the National Science Foundation (CHE1856437).
Research ethics: Not applicable.
Informed consent: Not applicable.
Author contributions: The author has accepted responsibility for the entire content of this manuscript and approved its submission.
Use of Large Language Models, AI and Machine Learning Tools: None declared.
Conflict of interest: The author states no conflict of interest.
Research funding: National Science Foundation CHE1856437.
Data availability: Not applicable.

References

1. Dirac, P. A. M.; Fowler, R. H. "The Fundamental Laws Necessary for the Mathematical Treatment of a Large Part of Physics and the Whole of Chemistry are thus Completely Known, and the Difficulty Lies Only in the Fact that Application of These Laws Leads to Equations that are too Complex to be Solved" Quantum Mechanics of Many-Electron Systems. *Proc. R. Soc. A* **1929**, *123*, 714–733. https://doi.org/10.1098/rspa.1929.0094.
2. Burke, K. Perspective on Density Functional Theory. *J. Chem. Phys.* **2012**, *136*, 150901. https://doi.org/10.1063/1.4704546.
3. Becke, A. D. Perspective: Fifty Years of Density-Functional Theory in Chemical Physics. *J. Chem. Phys.* **2014**, *140*, 18A301. https://doi.org/10.1063/1.4869598.
4. Jones, R. O. Density Functional Theory: Its Origins, Rise to Prominence, and Future. *Rev. Mod. Phys.* **2015**, *87*, 897–923. https://doi.org/10.1103/RevModPhys.87.897.
5. Karton, A. Quantum Mechanical Thermochemical Predictions 100 Years After the Schrodinger Equation. In *Annual Reports in Computational Chemistry*; Dixon, D. A., Ed.; Elsevier: Amsterdam, Vol. 18, 2022; pp 123–166.
6. Pople, J. A. Nobel Lecture: Quantum Chemical Models. *Rev. Mod. Phys.* **1999**, *71*, 1267–1274. https://doi.org/10.1103/RevModPhys.71.1267.
7. Wales, D. J. *Energy Landscapes*; Cambridge University Press: Cambridge, 2003.
8. Schlegel, H. B. Geometry Optimization. *Wiley Interdiscip. Rev. Comput. Mol. Sci.* **2011**, *1*, 790–809. https://doi.org/10.1002/wcms.34.
9. Fukui, K. The Path of Chemical-Reactions – The IRC Approach. *Acc. Chem. Res.* **1981**, *14*, 363–368. https://doi.org/10.1021/ar00072a001.
10. Born, M.; Oppenheimer, R. Zur Quantentheorie der Molekeln. *Ann. Phys.* **1927**, *389*, 457–484. https://doi.org/10.1002/andp.19273892002.
11. Sathyamurthy, N. Computational Fitting of Abinitio Potential-Energy Surfaces. *Comput. Phys. Rep.* **1985**, *3*, 1–70. https://doi.org/10.1016/0167-7977(85)90007-3.
12. Truhlar, D. G.; Steckler, R.; Gordon, M. S. Potential-Energy Surfaces for Polyatomic Reaction Dynamics. *Chem. Rev.* **1987**, *87*, 217–236. https://doi.org/10.1021/cr00077a011.
13. Schatz, G. C. The Analytical Representation of Electronic Potential-Energy Surfaces. *Rev. Mod. Phys.* **1989**, *61*, 669–688. https://doi.org/10.1103/revmodphys.61.669.
14. Hollebeek, T.; Ho, T. S.; Rabitz, H. Constructing Multidimensional Molecular Potential Energy Surfaces from Ab Initio Data. *Annu. Rev. Phys. Chem.* **1999**, *50*, 537–570. https://doi.org/10.1146/annurev.physchem.50.1.537.
15. Braams, B. J.; Bowman, J. M. Permutationally Invariant Potential Energy Surfaces in High Dimensionality. *Int. Rev. Phys. Chem.* **2009**, *28*, 577–606. https://doi.org/10.1080/01442350903234923.
16. Jiang, B.; Li, J.; Guo, H. Potential Energy Surfaces from High Fidelity Fitting of Ab Initio Points: The Permutation Invariant Polynomial – Neural Network Approach. *Int. Rev. Phys. Chem.* **2016**, *35*, 479–506. https://doi.org/10.1080/0144235x.2016.1200347.
17. Qu, C.; Yu, Q.; Bowman, J. M. Permutationally Invariant Potential Energy Surfaces. In *Annual Review of Physical Chemistry*; Johnson, M. A., Martinez, T. J., Eds.; Annual Reviews: Palo Alto, CA, Vol. 69, 2018; pp 151–175.
18. Dawes, R.; Quintas-Sánchez, E. The Construction of Ab Initio-Based Potential Energy Surfaces. In *Reviews in Computational Chemistry*; Parrill, A. L., Lipkowitz, K. B., Eds.; Wiley-Blackwell: Hoboken, NJ, Vol. 31, 2019; pp 199–263.

19. Shu, Y.; Varga, Z.; Jasper, A. W.; Garrett, B. C.; Espinosa-García, J.; Corchado, J. C.; Duchovic, R. J.; Volobuev, Y. L.; Lynch, G. C.; Yang, K. R.; Allison, T. C.; Wagner, A. F.; Truhlar, D. G. POTLIB: An Online Library of Potential Energy Surfaces. https://comp.chem.umn.edu/potlib/.
20. Behler, J. Four Generations of High-Dimensional Neural Network Potentials. *Chem. Rev.* **2021**, *121*, 10037–10072. https://doi.org/10.1021/acs.chemrev.0c00868.
21. Manzhos, S.; Carrington Jr., T. Neural Network Potential Energy Surfaces for Small Molecules and Reactions. *Chem. Rev.* **2021**, *121*, 10187–10217. https://doi.org/10.1021/acs.chemrev.0c00665.
22. Deringer, V. L.; Bartók, A. P.; Bernstein, N.; Wilkins, D. M.; Ceriotti, M.; Csányi, G. Gaussian Process Regression for Materials and Molecules. *Chem. Rev.* **2021**, *121*, 10073–10141. https://doi.org/10.1021/acs.chemrev.1c00022.
23. Kocer, E.; Ko, T. W.; Behler, J. Neural Network Potentials: A Concise Overview of Methods. *Annu. Rev. Phys. Chem.* **2022**, *73*, 163–186. https://doi.org/10.1146/annurev-physchem-082720-034254.
24. Pulay, P. Ab Initio Calculation of Force Constants and Equilibrium Geometries in Polyatomic Molecules. I. Theory. *Mol. Phys.* **1969**, *17*, 197–204. https://doi.org/10.1080/00268976900100941.
25. Pople, J. A.; Krishnan, R.; Schlegel, H. B.; Binkley, J. S. Derivative Studies in Hartree-Fock and Møller-Plesset Theories. *Int. J. Quantum Chem. Quantum Chem. Symp.* **1979**, *13*, 225–241.
26. Krishnan, R.; Schlegel, H. B.; Pople, J. A. Derivative Studies in Configuration-Interaction Theory. *J. Chem. Phys.* **1980**, *72*, 4654–4655. https://doi.org/10.1063/1.439708.
27. Handy, N. C.; Schaefer, H. F. On the Evaluation of Analytic Energy Derivatives for Correlated Wave-Functions. *J. Chem. Phys.* **1984**, *81*, 5031–5033. https://doi.org/10.1063/1.447489.
28. Kállay, M.; Gauss, J.; Szalay, P. G. Analytic First Derivatives for General Coupled-Cluster and Configuration Interaction Models. *J. Chem. Phys.* **2003**, *119*, 2991–3004. https://doi.org/10.1063/1.1589003.
29. Salter, E. A.; Trucks, G. W.; Bartlett, R. J. Analytic Energy Derivatives in Many-Body Methods. 1. 1st Derivatives. *J. Chem. Phys.* **1989**, *90*, 1752–1766. https://doi.org/10.1063/1.456069.
30. Pulay, P. Analytical Derivative Techniques and the Calculation of Vibrational Spectra. In *Modern Electronic Structure Theory*; Yarkony, D. R., Ed.; World Scientific Publishing: Singapore, 1995; p. 1191.
31. Pulay, P. Analytical Derivatives, Forces, Force Constants, Molecular Geometries, and Related Response Properties in Electronic Structure Theory. *Wiley Interdiscip. Rev. Comput. Mol. Sci.* **2014**, *4*, 169–181. https://doi.org/10.1002/wcms.1171.
32. Salter, E. A.; Bartlett, R. J. Analytic Energy Derivatives in Many-Body Methods. 2. 2nd Derivatives. *J. Chem. Phys.* **1989**, *90*, 1767–1773. https://doi.org/10.1063/1.456070.
33. Koch, H.; Jensen, H. J. A.; Jorgensen, P.; Helgaker, T.; Scuseria, G. E.; Schaefer, H. F. Coupled Cluster Energy Derivatives – Analytic Hessian for the Closed-Shell Coupled Cluster Singles and Doubles Wave-Function – Theory and Applications. *J. Chem. Phys.* **1990**, *92*, 4924–4940.
34. Gauss, J.; Stanton, J. F. Analytic CCSD(T) Second Derivatives. *Chem. Phys. Lett.* **1997**, *276*, 70–77. https://doi.org/10.1016/s0009-2614(97)88036-0.
35. Gauss, J.; Stanton, J. F. Analytic First and Second Derivatives for the CCSDT-N (N=1–3) Models: A First Step Towards the Efficient Calculation of CCSDT Properties. *Phys. Chem. Chem. Phys.* **2000**, *2*, 2047–2060. https://doi.org/10.1039/a909820h.
36. Friese, D. H.; Hättig, C.; Kossmann, J. Analytic Molecular Hessian Calculations for CC2 and MP2 Combined with the Resolution of Identity Approximation. *J. Chem. Theory Comput*. **2013**, *9*, 1469–1480. https://doi.org/10.1021/ct400034t.
37. Pulay, P. 2nd and 3rd Derivatives of Variational Energy Expressions – Application to Multiconfigurational Self-Consistent Field Wave-Functions. *J. Chem. Phys.* **1983**, *78*, 5043–5051. https://doi.org/10.1063/1.445372.
38. Hratchian, H. P.; Schlegel, H. B. Finding Minima, Transition States, and Following Reaction Pathways on Ab Initio Potential Energy Surfaces. In *Theory and Applications of Computational Chemistry: The First Forty Years*; Elsevier Science BV: Amsterdam, 2005; pp 195–249.
39. Maeda, S.; Harabuchi, Y. Exploring Paths of Chemical Transformations in Molecular and Periodic Systems: An Approach Utilizing Force. *Wiley Interdiscip. Rev. Comput. Mol. Sci.* **2021**, *11*, e1538. https://doi.org/10.1002/wcms.1538.
40. Dewyer, A. L.; Argüelles, A. J.; Zimmerman, P. M. Methods for Exploring Reaction Space in Molecular Systems. *Wiley Interdiscip. Rev. Comput. Mol. Sci.* **2018**, *8*, e1354. https://doi.org/10.1002/wcms.1354.
41. Pulay, P.; Fogarasi, G. Geometry Optimization in Redundant Internal Coordinates. *J. Chem. Phys.* **1992**, *96*, 2856–2860. https://doi.org/10.1063/1.462844.
42. Baker, J.; Kessi, A.; Delley, B. The Generation and Use of Delocalized Internal Coordinates in Geometry Optimization. *J. Chem. Phys.* **1996**, *105*, 192–212. https://doi.org/10.1063/1.471864.
43. Peng, C. Y.; Ayala, P. Y.; Schlegel, H. B.; Frisch, M. J. Using Redundant Internal Coordinates to Optimize Equilibrium Geometries and Transition States. *J. Comput. Chem.* **1996**, *17*, 49–56. https://doi.org/10.1002/(sici)1096-987x(19960115)17:1<49::aid-jcc5>3.3.co;2-#.
44. Hratchian, H. P.; Sonnenberg, J. L.; Frisch, M. J. Internal Coordinates for Exploring Potential Energy Surfaces Using a Generalized Coordinate Definition/Transformation Algorithm. *Abstr. Pap. Am. Chem. Soc.* **2011**, *241*.
45. Fletcher, R.; Reeves, C. M. Function Minimization by Conjugate Gradients. *Comput. J.* **1964**, *7*, 149–154.
46. Polak, E. *Computational Methods in Optimization: A Unified Approach*; Academic: New York, 1971.
47. Fletcher, R. *Practical Methods of Optimization*, 2nd ed.; Wiley: Chichester, 1987; p. xiv, 436.
48. Dennis, J. E.; Schnabel, R. B. *Numerical Methods for Unconstrained Optimization and Nonlinear Equations*; Prentice-Hall: Englewood Cliffs, NJ, 1983; p. xiii, 378.
49. Broyden, C. G. On the Convergence of a Class of Double Rank Minimization Algorithms. *J. Inst. Math. Appl.* **1970**, *6*, 76–90. https://doi.org/10.1093/imamat/6.1.76.

50. Fletcher, R. A New Approach to Variable Metric Algorithms. *Comput. J.* **1970**, *13*, 317–322. https://doi.org/10.1093/comjnl/13.3.317.
51. Goldfarb, D. A Family of Variable Metric Methods Derived by Variational Means. *Math. Comput.* **1970**, *24*, 23–26. https://doi.org/10.1090/s0025-5718-1970-0258249-6.
52. Shanno, D. F. Conditioning of Quasi-Newton Methods for Functional Minimization. *Math. Comput.* **1970**, *24*, 647–657. https://doi.org/10.2307/2004840.
53. Wolfe, P. Convergence Conditions for Ascent Methods. *SIAM Rev.* **1969**, *11*, 226–235. https://doi.org/10.1137/1011036.
54. Liu, D. C.; Nocedal, J. On the Limited Memory BFGS Method for Large-Scale Optimization. *Math. Program.* **1989**, *45*, 503–528. https://doi.org/10.1007/bf01589116.
55. Csaszar, P.; Pulay, P. Geometry Optimization by Direct Inversion in the Iterative Subspace. *J. Mol. Struct.* **1984**, *114*, 31–34. https://doi.org/10.1016/s0022-2860(84)87198-7.
56. Li, X. S.; Frisch, M. J. Energy-Represented Direct Inversion in the Iterative Subspace Within a Hybrid Geometry Optimization Method. *J. Chem. Theory Comput*. **2006**, *2*, 835–839. https://doi.org/10.1021/ct050275a.
57. Denzel, A.; Kästner, J. Gaussian Process Regression for Geometry Optimization. *J. Chem. Phys.* **2018**, *148*, 094114. https://doi.org/10.1063/1.5017103.
58. Meyer, R.; Hauser, A. W. Geometry Optimization Using Gaussian Process Regression in Internal Coordinate Systems. *J. Chem. Phys.* **2020**, *152*, 084112. https://doi.org/10.1063/1.5144603.
59. Raggi, G.; Galván, I. F.; Ritterhoff, C. L.; Vacher, M.; Lindh, R. Restricted-Variance Molecular Geometry Optimization Based on Gradient-Enhanced Kriging. *J. Chem. Theory Comput*. **2020**, *16*, 3989–4001. https://doi.org/10.1021/acs.jctc.0c00257.
60. Teng, C.; Huang, D.; Bao, J. L. A Spur to Molecular Geometry Optimization: Gradient-Enhanced Universal Kriging with On-the-Fly Adaptive Ab Initio Prior Mean Functions in Curvilinear Coordinates. *J. Chem. Phys.* **2023**, *158*, 024112. https://doi.org/10.1063/5.0133675.
61. Banerjee, A.; Adams, N.; Simons, J.; Shepard, R. Search for Stationary-Points on Surface. *J. Phys. Chem.* **1985**, *89*, 52–57. https://doi.org/10.1021/j100247a015.
62. Besalu, E.; Bofill, J. M. On the Automatic Restricted-Step Rational-Function-Optimization Method. *Theor. Chem. Acc.* **1998**, *100*, 265–274. https://doi.org/10.1007/s002140050387.
63. Anglada, J. M.; Bofill, J. M. On the Restricted Step Method Coupled with the Augmented Hessian for the Search of Stationary Points of Any Continuous Function. *Int. J. Quantum Chem.* **1997**, *62*, 153–165. https://doi.org/10.1002/(sici)1097-461x(1997)62:2<153::aid-qua3>3.0.co;2-v.
64. Levine, D. S.; Shuaibi, M.; Spotte-Smith, E. W. C.; Taylor, M. G.; Hasyim, M. R.; Michel, K.; Batatia, I.; Csányi, G.; Dzamba, M.; Eastman, P.; Frey, N. C.; Fu, X.; Gharakhanyan, V.; Krishnapriyan, A. S.; Rackers, J. A.; Raja, S.; Rizvi, A.; Rosen, A. S.; Ulissi, Z.; Vargas, S.; Zitnick, C. L.; Blau, S. M.; Wood, B. M. The Open Molecules 2025 (OMol25) Dataset, Evaluations, and Models. arXiv:2505.08762v1 **2025**. https://doi.org/10.48550/arXiv.2505.08762.
65. Smith, J. S.; Isayev, O.; Roitberg, A. E. ANI-1, A Data Set of 20 Million Calculated Off-Equilibrium Conformations for Organic Molecules. *Sci. Data* **2017**, *4*, 170193. https://doi.org/10.1038/sdata.2017.193.
66. Smith, J. S.; Zubatyuk, R.; Nebgen, B.; Lubbers, N.; Barros, K.; Roitberg, A. E.; Isayev, O.; Tretiak, S. The ANI-1ccx and ANI-1x Data Sets, Coupled-Cluster and Density Functional Theory Properties for Molecules. *Sci. Data* **2020**, *7*, 134. https://doi.org/10.1038/s41597-020-0473-z.
67. Nakata, M.; Shimazaki, T. PubChemQC Project: A Large-Scale First-Principles Electronic Structure Database for Data-Driven Chemistry. *J. Chem. Inf. Model.* **2017**, *57*, 1300–1308. https://doi.org/10.1021/acs.jcim.7b00083.
68. Keith, J. A.; Vassilev-Galindo, V.; Cheng, B. Q.; Chmiela, S.; Gastegger, M.; Mueller, K. R.; Tkatchenko, A. Combining Machine Learning and Computational Chemistry for Predictive Insights into Chemical Systems. *Chem. Rev.* **2021**, *121*, 9816–9872. https://doi.org/10.1021/acs.chemrev.1c00107.
69. Komornicki, A.; Ishida, K.; Morokuma, K.; Ditchfield, R.; Conrad, M. Efficient Determination and Characterization of Transition-States Using Ab Initio Methods. *Chem. Phys. Lett.* **1977**, *45*, 595–602. https://doi.org/10.1016/0009-2614(77)80099-7.
70. Cerjan, C. J.; Miller, W. H. On Finding Transition States. *J. Chem. Phys.* **1981**, *75*, 2800–2806. https://doi.org/10.1063/1.442352.
71. Simons, J.; Jorgensen, P.; Taylor, H.; Ozment, J. Walking on Potential-Energy Surfaces. *J. Phys. Chem.* **1983**, *87*, 2745–2753. https://doi.org/10.1021/j100238a013.
72. Simons, J.; Nichols, J. Strategies for Walking on Potential-Energy Surfaces Using Local Quadratic Approximations. *Int. J. Quantum Chem.* **1990**, *Suppl. 24*, 263–276. https://doi.org/10.1002/qua.560382427.
73. Samanta, A.; E, W. Atomistic Simulations of Rare Events Using Gentlest Ascent Dynamics. *J. Chem. Phys.* **2012**, *136*, 124104. https://doi.org/10.1063/1.3692803.
74. Henkelman, G.; Jonsson, H. A Dimer Method for Finding Saddle Points on High Dimensional Potential Surfaces Using Only First Derivatives. *J. Chem. Phys.* **1999**, *111*, 7010–7022. https://doi.org/10.1063/1.480097.
75. Kaestner, J.; Sherwood, P. Superlinearly Converging Dimer Method for Transition State Search. *J. Chem. Phys.* **2008**, *128*, 014106. https://doi.org/10.1063/1.2815812.
76. Shang, C.; Liu, Z. P. Constrained Broyden Minimization Combined with the Dimer Method for Locating Transition State of Complex Reactions. *J. Chem. Theory Comput*. **2010**, *6*, 1136–1144. https://doi.org/10.1021/ct9005147.
77. Rothman, M. J.; Lohr, L. L. Analysis of an Energy Minimization Method for Locating Transition-States on Potential-Energy Hypersurfaces. *Chem. Phys. Lett.* **1980**, *70*, 405–409. https://doi.org/10.1016/0009-2614(80)85361-9.

78. Burkert, U.; Allinger, N. L. Pitfalls in the Use of the Torion Angle Driving Method for the Calculation of Conformational Interconversions. *J. Comput. Chem.* **1982**, *3*, 40–46. https://doi.org/10.1002/jcc.540030108.
79. Quapp, W.; Hirsch, M.; Imig, O.; Heidrich, D. Searching for Saddle Points of Potential Energy Surfaces by Following a Reduced Gradient. *J. Comput. Chem.* **1998**, *19*, 1087–1100. https://doi.org/10.1002/(sici)1096-987x(19980715)19:9<1087::aid-jcc9>3.3.co;2-s.
80. Crehuet, R.; Bofill, J. M.; Anglada, J. M. A New Look at the Reduced-Gradient-Following Path. *Theor. Chem. Acc.* **2002**, *107*, 130–139. https://doi.org/10.1007/s00214-001-0306-x.
81. Quapp, W. Newton Trajectories in the Curvilinear Metric of Internal Coordinates. *J. Math. Chem.* **2004**, *36*, 365–379. https://doi.org/10.1023/b:jomc.0000044524.48281.2d.
82. Liu, Y. L.; Burger, S. K.; Ayers, P. W. Newton Trajectories for Finding Stationary Points on Molecular Potential Energy Surfaces. *J. Math. Chem.* **2011**, *49*, 1915–1927. https://doi.org/10.1007/s10910-011-9864-x.
83. Hoffman, D. K.; Nord, R. S.; Ruedenberg, K. Gradient Extremals. *Theor. Chim. Acta* **1986**, *69*, 265–279. https://doi.org/10.1007/bf00527704.
84. Sun, J. Q.; Ruedenberg, K. Gradient Extremals and Steepest Descent Lines on Potential-Energy Surfaces. *J. Chem. Phys.* **1993**, *98*, 9707–9714. https://doi.org/10.1063/1.464349.
85. Jorgensen, P.; Jensen, H. J. A.; Helgaker, T. A Gradient Extremal Walking Algorithm. *Theor. Chim. Acta* **1988**, *73*, 55–65. https://doi.org/10.1007/bf00526650.
86. Schlegel, H. B. Following Gradient Extremal Paths. *Theor. Chim. Acta* **1992**, *83*, 15–20. https://doi.org/10.1007/bf01113240.
87. Halgren, T.; Lipscomb, W. N. The Synchronous-Transit Method for Determining Reaction Pathways and Locating Molecular Transition States. *Chem. Phys. Lett.* **1977**, *49*, 225–232. https://doi.org/10.1016/0009-2614(77)80574-5.
88. Peng, C. Y.; Schlegel, H. B. Combining Synchronous Transit and Quasi-Newton Methods to Find Transition-States. *Isr. J. Chem.* **1993**, *33*, 449–454.
89. Bofill, J. M. Updated Hessian Matrix and the Restricted Step Method for Locating Transition Structures. *J. Comput. Chem.* **1994**, *15*, 1–11. https://doi.org/10.1002/jcc.540150102.
90. Baker, J. An Algorithm for the Location of Transition-States. *J. Comput. Chem.* **1986**, *7*, 385–395. https://doi.org/10.1002/jcc.540070402.
91. Culot, P.; Dive, G.; Nguyen, V. H.; Ghuysen, J. M. A Quasi-Newton Algorithm for 1st-Order Saddle-Point Location. *Theor. Chim. Acta* **1992**, *82*, 189–205. https://doi.org/10.1007/bf01113251.
92. Elber, R.; Karplus, M. A Method for Determining Reaction Paths in Large Molecules – Application to Myoglobin. *Chem. Phys. Lett.* **1987**, *139*, 375–380. https://doi.org/10.1016/0009-2614(87)80576-6.
93. Jónsson, H.; Mills, G.; Jacobsen, W. Nudged Elastic Band Method for Finding Minimum Energy Paths of Transitions. In *Classical and Quantum Dynamics in Condensed Phase Simulations*; Berne, B. J.; Cicotti, G.; Coker, D. F., Eds.; World Scientific: Singapore, 1998; p. 385.
94. Henkelman, G.; Jonsson, H. Improved Tangent Estimate in the Nudged Elastic Band Method for Finding Minimum Energy Paths and Saddle Points. *J. Chem. Phys.* **2000**, *113*, 9978–9985. https://doi.org/10.1063/1.1323224.
95. Trygubenko, S. A.; Wales, D. J. A Doubly Nudged Elastic Band Method for Finding Transition States. *J. Chem. Phys.* **2004**, *120*, 2082–2094. https://doi.org/10.1063/1.1636455.
96. E, W. N.; Ren, W. Q.; Vanden-Eijnden, E. String Method for the Study of Rare Events. *Phys. Rev. B* **2002**, *66*, 052301. https://doi.org/10.1103/PhysRevB.66.052301.
97. Burger, S. K.; Yang, W. T. Quadratic String Method for Determining the Minimum-Energy Path Based on Multiobjective Optimization. *J. Chem. Phys.* **2006**, *124*, 054109. https://doi.org/10.1063/1.2163875.
98. Ren, W.; Vanden-Eijnden, E. A Climbing String Method for Saddle Point Search. *J. Chem. Phys.* **2013**, *138*, 134105. https://doi.org/10.1063/1.4798344.
99. Zimmerman, P. M. Growing String Method with Interpolation and Optimization in Internal Coordinates: Method and Examples. *J. Chem. Phys.* **2013**, *138*, 184102. https://doi.org/10.1063/1.4804162.
100. Behn, A.; Zimmerman, P. M.; Bell, A. T.; Head-Gordon, M. Efficient Exploration of Reaction Paths via a Freezing String Method. *J. Chem. Phys.* **2011**, *135*, 224108. https://doi.org/10.1063/1.3664901.
101. Ayala, P. Y.; Schlegel, H. B. A Combined Method for Determining Reaction Paths, Minima, and Transition State Geometries. *J. Chem. Phys.* **1997**, *107*, 375–384. https://doi.org/10.1063/1.474398.
102. Plessow, P. Reaction Path Optimization without NEB Springs or Interpolation Algorithms. *J. Chem. Theory Comput*. **2013**, *9*, 1305–1310. https://doi.org/10.1021/ct300951j.
103. Denzel, A.; Haasdonk, B.; Kästner, J. Gaussian Process Regression for Minimum Energy Path Optimization and Transition State Search. *J. Phys. Chem. A* **2019**, *123*, 9600–9611. https://doi.org/10.1021/acs.jpca.9b08239.
104. Ishida, K.; Morokuma, K.; Komornicki, A. The Intrinsic Reaction Coordinate. An Ab Initio Calculation for HNC → HCN and H^- + CH_4 → CH_4 + H^-. *J. Chem. Phys.* **1977**, *66*, 2153–2156. https://doi.org/10.1063/1.434152.
105. Page, M.; Doubleday, C.; McIver, J. W. Following Steepest Descent Reaction Paths – The Use of Higher Energy Derivatives with Abinitio Electronic-Structure Methods. *J. Chem. Phys.* **1990**, *93*, 5634–5642. https://doi.org/10.1063/1.459634.
106. Sun, J. Q.; Ruedenberg, K. Quadratic Steepest Descent on Potential-Energy Surfaces. 2. Reaction-Path Following Without Analytic Hessians. *J. Chem. Phys.* **1993**, *99*, 5269–5275. https://doi.org/10.1063/1.465995.
107. Baldridge, K. K.; Gordon, M. S.; Steckler, R.; Truhlar, D. G. Ab Initio Reaction Paths and Direct Dynamics Calculations. *J. Phys. Chem.* **1989**, *93*, 5107–5119. https://doi.org/10.1021/j100350a018.

108. Gordon, M. S.; Chaban, G.; Taketsugu, T. Interfacing Electronic Structure Theory with Dynamics. *J. Phys. Chem.* **1996**, *100*, 11512–11525. https://doi.org/10.1021/jp953371o.
109. Burger, S. K.; Yang, W. T. A Combined Explicit-Implicit Method for High Accuracy Reaction Path Integration. *J. Chem. Phys.* **2006**, *124*, 224102. https://doi.org/10.1163/1.2202830.
110. Gonzalez, C.; Schlegel, H. B. An Improved Algorithm for Reaction-Path Following. *J. Chem. Phys.* **1989**, *90*, 2154–2161. https://doi.org/10.1063/1.456010.
111. Gonzalez, C.; Schlegel, H. B. Improved Algorithms for Reaction-Path Following – Higher-Order Implicit Algorithms. *J. Chem. Phys.* **1991**, *95*, 5853–5860. https://doi.org/10.1063/1.461606.
112. Hratchian, H. P.; Schlegel, H. B. Using Hessian Updating to Increase the Efficiency of a Hessian Based Predictor-Corrector Reaction Path Following Method. *J. Chem. Theory Comput.* **2005**, *1*, 61–69. https://doi.org/10.1021/ct0499783.
113. Hratchian, H. P.; Frisch, M. J.; Schlegel, H. B. Steepest Descent Reaction Path Integration Using a First-Order Predictor-Corrector Method. *J. Chem. Phys.* **2010**, *133*, 224101. https://doi.org/10.1063/1.3514202.
114. Miller, W. H.; Handy, N. C.; Adams, J. E. Reaction-Path Hamiltonian for Polyatomic-Molecules. *J. Chem. Phys.* **1980**, *72*, 99–112. https://doi.org/10.1063/1.438959.
115. Kraka, E. Reaction Path Hamiltonian and the Unified Reaction Valley Approach. *Wiley Interdiscip. Rev. Comput. Mol. Sci.* **2011**, *1*, 531–556. https://doi.org/10.1002/wcms.65.
116. Zou, W. L.; Sexton, T.; Kraka, E.; Freindorf, M.; Cremer, D. A New Method for Describing the Mechanism of a Chemical Reaction Based on the Unified Reaction Valley Approach. *J. Chem. Theory Comput*. **2016**, *12*, 650–663. https://doi.org/10.1021/acs.jctc.5b01098.
117. Kraka, E.; Zou, W. L.; Tao, Y. W.; Freindorf, M. Exploring the Mechanism of Catalysis with the Unified Reaction Valley Approach (URVA)-A Review. *Catalysts* **2020**, *10*, 691. https://doi.org/10.3390/catal10060691.
118. Bakken, V.; Danovich, D.; Shaik, S.; Schlegel, H. B. A Single Transition State Serves Two Mechanisms: An Ab Initio Classical Trajectory Study of the Electron Transfer and Substitution Mechanisms in Reactions of Ketyl Radical Anions with Alkyl Halides. *J. Am. Chem. Soc.* **2001**, *123*, 130–134. https://doi.org/10.1021/ja002799k.
119. Ess, D. H.; Wheeler, S. E.; Iafe, R. G.; Xu, L.; Çelebi-Ölcüm, N.; Houk, K. N. Bifurcations on Potential Energy Surfaces of Organic Reactions. *Angew. Chem., Int. Ed.* **2008**, *47*, 7592–7601. https://doi.org/10.1002/anie.200800918.
120. Hong, Y. J.; Tantillo, D. J. A Potential Energy Surface Bifurcation in Terpene Biosynthesis. *Nat. Chem.* **2009**, *1*, 384–389. https://doi.org/10.1038/nchem.287.
121. Pham, H. V.; Houk, K. N. Diels-Alder Reactions of Allene with Benzene and Butadiene: Concerted, Stepwise, and Ambimodal Transition States. *J. Org. Chem.* **2014**, *79*, 8968–8976. https://doi.org/10.1021/jo502041f.
122. Hare, S. R.; Tantillo, D. J. Post-Transition State Bifurcations Gain Momentum – Current State of the Field. *Pure Appl. Chem.* **2017**, *89*, 679–698. https://doi.org/10.1515/pac-2017-0104.
123. Jamieson, C. S.; Sengupta, A.; Houk, K. N. Cycloadditions of Cyclopentadiene and Cycloheptatriene with Tropones: All Endo- 6+4 Cycloadditions are Ambimodal. *J. Am. Chem. Soc.* **2021**, *143*, 3918–3926. https://doi.org/10.1021/jacs.0c13401.
124. Zhou, Q. Y.; Thogersen, M. K.; Rezayee, N. M.; Jorgensen, K. A.; Houk, K. N. Ambimodal Bispericyclic 6+4/4+6 Transition State Competes with Diradical Pathways in the Cycloheptatriene Dimerization: Dynamics and Experimental Characterization of Thermal Dimers. *J. Am. Chem. Soc.* **2022**, *144*, 22251–22261. https://doi.org/10.1021/jacs.2c10407.
125. Bofill, J. M.; Quapp, W. Analysis of the Valley-Ridge Inflection Points Through the Partitioning Technique of the Hessian Eigenvalue Equation. *J. Math. Chem.* **2013**, *51*, 1099–1115. https://doi.org/10.1007/s10910-012-0134-3.
126. Lee, S.; Goodman, J. M. Rapid Route-Finding for Bifurcating Organic Reactions. *J. Am. Chem. Soc.* **2020**, *142*, 9210–9219. https://doi.org/10.1021/jacs.9b13449.
127. Bharadwaz, P.; Maldonado-Domínguez, M.; Srnec, M. Bifurcating Reactions: Distribution of Products from Energy Distribution in a Shared Reactive Mode. *Chem. Sci.* **2021**, *12*, 12682–12694. https://doi.org/10.1039/d1sc02826j.
128. Carpenter, B. K. Prediction of Kinetic Product Ratios: Investigation of a Dynamically Controlled Case. *J. Phys. Chem. A* **2023**, *127*, 224–239. https://doi.org/10.1021/acs.jpca.2c08301.
129. Kuan, K. Y.; Hsu, C. P. Predicting Selectivity with a Bifurcating Surface: Inaccurate Model or Inaccurate Statistics of Dynamics? *J. Phys. Chem. A* **2024**, *128*, 6798–6805. https://doi.org/10.1021/acs.jpca.4c04039.
130. Murakami, T.; Kikuma, Y.; Hayashi, D.; Ibuki, S.; Nakagawa, S.; Ueno, H.; Takayanagi, T. Molecular Dynamics Simulation Study of Post-Transition State Bifurcation: A Case Study on the Ambimodal Transition State of dipolar/Diels-Alder Cycloaddition. *J. Phys. Org. Chem.* **2024**, *37*, e4611. https://doi.org/10.1002/poc.4611.
131. Shin, W.; Hou, Y. N.; Wang, X.; Yang, Z. J. Interplay Between Energy and Entropy Mediates Ambimodal Selectivity of Cycloadditions. *J. Chem. Theory Comput*. **2024**, *20*, 10942–10951. https://doi.org/10.1021/acs.jctc.4c01138.
132. Baker, J.; Gill, P. M. W. An Algorithm for the Location of Branching Points on Reaction Paths. *J. Comput. Chem.* **1988**, *9*, 465–475. https://doi.org/10.1002/jcc.540090505.
133. Ito, T.; Harabuchi, Y.; Maeda, S. AFIR Explorations of Transition States of Extended Unsaturated Systems: Automatic Location of Ambimodal Transition States. *Phys. Chem. Chem. Phys.* **2020**, *22*, 13942–13950. https://doi.org/10.1039/d0cp02379e.
134. Chuang, H. H.; Tantillo, D. J.; Hsu, C. P. Construction of Two-Dimensional Potential Energy Surfaces of Reactions with Post-Transition-State Bifurcations. *J. Chem. Theory Comput*. **2020**, *16*, 4050–4060. https://doi.org/10.1021/acs.jctc.0c00172.
135. Maeda, S.; Harabuchi, Y.; Ono, Y.; Taketsugu, T.; Morokuma, K. Intrinsic Reaction Coordinate: Calculation, Bifurcation, and Automated Search. *Int. J. Quantum Chem.* **2015**, *115*, 258–269. https://doi.org/10.1002/qua.24757.

136. Aarabi, M.; Pandey, A.; Poirier, B. "On-the-Fly" Crystal: How to Reliably and Automatically Characterize and Construct Potential Energy Surfaces. *J. Comput. Chem.* **2024**, *45*, 1261–1278. https://doi.org/10.1002/jcc.27324.
137. Simm, G. N.; Vaucher, A. C.; Reiher, M. Exploration of Reaction Pathways and Chemical Transformation Networks. *J. Phys. Chem. A* **2019**, *123*, 385–399. https://doi.org/10.1021/acs.jpca.8b10007.
138. Unsleber, J. P.; Reiher, M. The Exploration of Chemical Reaction Networks. In *Annual Review of Physical Chemistry*; Johnson, M. A., Martinez, T. J., Eds.; Annual Reviews: Palo Alto, CA, Vol. 71, 2020; pp 121–142.
139. Habershon, S. Sampling Reactive Pathways with Random Walks in Chemical Space: Applications to Molecular Dissociation and Catalysis. *J. Chem. Phys.* **2015**, *143*, 094106. https://doi.org/10.1063/1.4929992.
140. Habershon, S. Automated Prediction of Catalytic Mechanism and Rate Law Using Graph-Based Reaction Path Sampling. *J. Chem. Theory Comput.* **2016**, *12*, 1786–1798. https://doi.org/10.1021/acs.jctc.6b00005.
141. Gao, C. W.; Allen, J. W.; Green, W. H.; West, R. H. Reaction Mechanism Generator: Automatic Construction of Chemical Kinetic Mechanisms. *Comput. Phys. Commun.* **2016**, *203*, 212–225. https://doi.org/10.1016/j.cpc.2016.02.013.
142. Grambow, C. A.; Pattanaik, L.; Green, W. H. Reactants, Products, and Transition States of Elementary Chemical Reactions Based on Quantum Chemistry. *Sci. Data* **2020**, *7*, 137. https://doi.org/10.1038/s41597-020-0460-4.
143. Wang, L. P.; McGibbon, R. T.; Pande, V. S.; Martinez, T. J. Automated Discovery and Refinement of Reactive Molecular Dynamics Pathways. *J. Chem. Theory Comput.* **2016**, *12*, 638–649. https://doi.org/10.1021/acs.jctc.5b00830.
144. Meuwly, M. Machine Learning for Chemical Reactions. *Chem. Rev.* **2021**, *121*, 10218–10239. https://doi.org/10.1021/acs.chemrev.1c00033.
145. Zener, C. Non-Adiabatic Crossing of Energy Levels. *Proc. R. Soc. A* **1932**, *137*, 696–702.
146. Teller, E. The Crossing of Potential Surfaces. *J. Phys. Chem.* **1937**, *41*, 109–116. https://doi.org/10.1021/j150379a010.
147. Matsika, S. Electronic Structure Methods for the Description of Nonadiabatic Effects and Conical Intersections. *Chem. Rev.* **2021**, *121*, 9407–9449. https://doi.org/10.1021/acs.chemrev.1c00074.
148. Keal, T. W.; Koslowski, A.; Thiel, W. Comparison of Algorithms for Conical Intersection Optimisation Using Semiempirical Methods. *Theor. Chem. Acc.* **2007**, *118*, 837–844. https://doi.org/10.1007/s00214-007-0331-5.
149. Levine, B. G.; Coe, J. D.; Martinez, T. J. Optimizing Conical Intersections Without Derivative Coupling Vectors: Application to Multistate Multireference Second-Order Perturbation Theory (MS-CASPT2). *J. Phys. Chem. B* **2008**, *112*, 405–413. https://doi.org/10.1021/jp0761618.
150. Ciminelli, C.; Granucci, G.; Persico, M. The Photoisomerization Mechanism of Azobenzene: A Semiclassical Simulation of Nonadiabatic Dynamics. *Chem. Eur. J.* **2004**, *10*, 2327–2341. https://doi.org/10.1002/chem.200305415.
151. Sicilia, F.; Blancafort, L.; Bearpark, M. J.; Robb, M. A. New Algorithms for Optimizing and Linking Conical Intersection Points. *J. Chem. Theory Comput.* **2008**, *4*, 257–266. https://doi.org/10.1021/ct7002435.
152. Bearpark, M. J.; Robb, M. A.; Schlegel, H. B. A Direct Method for the Location of the Lowest Energy Point on a Potential Surface Crossing. *Chem. Phys. Lett.* **1994**, *223*, 269–274.
153. Ruiz-Barragan, S.; Robb, M. A.; Blancafort, L. Conical Intersection Optimization Based on a Double Newton-Raphson Algorithm Using Composed Steps. *J. Chem. Theory Comput.* **2013**, *9*, 1433–1442. https://doi.org/10.1021/ct301059t.
154. Harabuchi, Y.; Taketsugu, T.; Maeda, S. Combined Gradient Projection/Single Component Artificial Force Induced Reaction (GP/SC-AFIR) Method for an Efficient Search of Minimum Energy Conical Intersection (MECI) Geometries. *Chem. Phys. Lett.* **2017**, *674*, 141–145. https://doi.org/10.1016/j.cplett.2017.02.069.
155. Anglada, J. M.; Bofill, J. M. A Reduced-Restricted-Quasi-Newton-Raphson Method for Locating and Optimizing Energy Crossing Points Between Two Potential Energy Surfaces. *J. Comput. Chem.* **1997**, *18*, 992–1003. https://doi.org/10.1002/(sici)1096-987x(199706)18:8<992::aid-jcc3>3.0.co;2-l.
156. Koga, N.; Morokuma, K. Determination of the Lowest Energy Point on the Crossing Seam Between 2 Potential Surfaces Using the Energy Gradient. *Chem. Phys. Lett.* **1985**, *119*, 371–374. https://doi.org/10.1016/0009-2614(85)80436-x.
157. Manaa, M. R.; Yarkony, D. R. On the Intersection of 2 Potential-Energy Surfaces of the Same Symmetry – Systematic Characterization Using a Lagrange Multiplier Constrained Procedure. *J. Chem. Phys.* **1993**, *99*, 5251–5256. https://doi.org/10.1063/1.465993.
158. García, J. S.; Maskri, R.; Mitrushchenkov, A.; Joubert-Doriol, L. Optimizing Conical Intersections Without Explicit Use of Non-Adiabatic Couplings. *J. Chem. Theory Comput.* **2024**, *20*, 5643–5654. https://doi.org/10.1021/acs.jctc.4c00326.
159. Ragazos, I. N.; Robb, M. A.; Bernardi, F.; Olivucci, M. Optimization and Characterization of the Lowest Energy Point on a Conical Intersection Using an MC-SCF Lagrangian. *Chem. Phys. Lett.* **1992**, *197*, 217–223. https://doi.org/10.1016/0009-2614(92)85758-3.
160. Farazdel, A.; Dupuis, M. On the Determination of the Minimum on the Crossing Seam of 2 Potential-Energy Surfaces. *J. Comput. Chem.* **1991**, *12*, 276–282. https://doi.org/10.1002/jcc.540120219.
161. Yarkony, D. R. On the Characterization of Regions of Avoided Surface Crossings Using an Analytic Gradient Based Method. *J. Chem. Phys.* **1990**, *92*, 2457–2463. https://doi.org/10.1063/1.457988.
162. Pandey, A.; Poirier, B.; Liang, R. B. Development of Parallel On-the-Fly Crystal Algorithm for Global Exploration of Conical Intersection Seam Space. *J. Chem. Theory Comput.* **2024**, *20*, 4778–4789. https://doi.org/10.1021/acs.jctc.4c00292.
163. Pieri, E.; Lahana, D.; Chang, A. M.; Aldaz, C. R.; Thompson, K. C.; Martínez, T. J. The Non-Adiabatic Nanoreactor: Towards the Automated Discovery of Photochemistry. *Chem. Sci.* **2021**, *12*, 7294–7307. https://doi.org/10.1039/d1sc00775k.
164. Ben-Nun, M.; Quenneville, J.; Martínez, T. J. Ab Initio Multiple Spawning: Photochemistry from First Principles Quantum Molecular Dynamics. *J. Phys. Chem. A* **2000**, *104*, 5161–5175. https://doi.org/10.1021/jp994174i.
165. Bunker, D. L. Classical Trajectory Methods. *Math. Comput. Phys.* **1971**, *10*, 287–325. https://doi.org/10.1016/b978-0-12-460810-8.50012-9.

166. Raff, L. M.; Thompson, D. L. The Classical Trajectory Approach to Reactive Scattering. In *Theory of Chemical Reaction Dynamics*; Baer, M., Ed.; CRC Press: Boca Raton, 1985.
167. Sewell, T. D.; Thompson, D. L. Classical Trajectory Methods for Polyatomic Molecules. *Int. J. Mod. Phys. B* **1997**, *11*, 1067–1112. https://doi.org/10.1142/s0217979297000551.
168. Sun, L. P.; Hase, W. L. Born-Oppenheimer Direct Dynamics Classical Trajectory Simulations. In *Reviews in Computational Chemistry*; Lipkowitz, K. B., Larter, R., Cundari, T. R., Boyd, D. B., Eds.; Wiley Blackwell: Hoboken, NJ, Vol. 19, 2003; pp 79–146.
169. Pratihar, S.; Ma, X. Y.; Homayoon, Z.; Barnes, G. L.; Hase, W. L. Direct Chemical Dynamics Simulations. *J. Am. Chem. Soc.* **2017**, *139*, 3570–3590. https://doi.org/10.1021/jacs.6b12017.
170. Verlet, L. Computer Experiments on Classical Fluids. I. Thermodynamical Properties of Lennard-Jones Molecules. *Phys. Rev.* **1967**, *159*, 98–103. https://doi.org/10.1103/physrev.159.98.
171. Yoshida, H. Construction of Higher-Order Symplectic Integrators. *Phys. Lett. A* **1990**, *150*, 262–268. https://doi.org/10.1016/0375-9601(90)90092-3.
172. Odell, A.; Delin, A.; Johansson, B.; Bock, N.; Challacombe, M.; Niklasson, A. M. N. Higher-Order Symplectic Integration in Born-Oppenheimer Molecular Dynamics. *J. Chem. Phys.* **2009**, *131*, 244106. https://doi.org/10.1063/1.3268338.
173. Millam, J. M.; Bakken, V.; Chen, W.; Hase, W. L.; Schlegel, H. B. Ab Initio Classical Trajectories on the Born-Oppenheimer Surface: Hessian-Based Integrators Using Fifth-Order Polynomial and Rational Function Fits. *J. Chem. Phys.* **1999**, *111*, 3800–3805. https://doi.org/10.1063/1.480037.
174. Bakken, V.; Millam, J. M.; Schlegel, H. B. Ab Initio Classical Trajectories on the Born-Oppenheimer Surface: Updating Methods for Hessian-Based Integrators. *J. Chem. Phys.* **1999**, *111*, 8773–8777. https://doi.org/10.1063/1.480224.
175. Wu, H.; Rahman, M.; Wang, J.; Louderaj, U.; Hase, W. L.; Zhuang, Y. Higher-Accuracy Schemes for Approximating the Hessian from Electronic Structure Calculations in Chemical Dynamics Simulations. *J. Chem. Phys.* **2010**, *133*, 074101. https://doi.org/10.1063/1.3407922.
176. Niklasson, A. M. N. Extended Lagrangian Born-Oppenheimer Molecular Dynamics: From Density Functional Theory to Charge Relaxation Models. *Eur. J. Phys. B* **2021**, *94*, 164. https://doi.org/10.1140/epjb/s10051-021-00151-6.
177. Tuckerman, M. E. Ab Initio Molecular Dynamics: Basic Concepts, Current Trends and Novel Applications. *J. Phys. Condens. Matter* **2002**, *14*, R1297–R1355. https://doi.org/10.1088/0953-8984/14/50/202.
178. Hutter, J. Car-Parrinello Molecular Dynamics. *Wiley Interdiscip. Rev. Comput. Mol. Sci.* **2012**, *2*, 604–612. https://doi.org/10.1002/wcms.90.
179. Car, R.; Parrinello, M. Unified Approach for Molecular-Dynamics and Density-Functional Theory. *Phys. Rev. Lett.* **1985**, *55*, 2471–2474. https://doi.org/10.1103/PhysRevLett.55.2471.
180. Schlegel, H. B.; Millam, J. M.; Iyengar, S. S.; Voth, G. A.; Daniels, A. D.; Scuseria, G. E.; Frisch, M. J. Ab Initio Molecular Dynamics: Propagating the Density Matrix with Gaussian Orbitals. *J. Chem. Phys.* **2001**, *114*, 9758–9763. https://doi.org/10.1063/1.1372182.
181. Iyengar, S. S.; Schlegel, H. B.; Millam, J. M.; Voth, G. A.; Scuseria, G. E.; Frisch, M. J. Ab Initio Molecular Dynamics: Propagating the Density Matrix with Gaussian Orbitals. II. Generalizations Based on Mass-Weighting, Idempotency, Energy Conservation and Choice of Initial Conditions. *J. Chem. Phys.* **2001**, *115*, 10291–10302. https://doi.org/10.1063/1.1416876.
182. Schlegel, H. B.; Iyengar, S. S.; Li, X. S.; Millam, J. M.; Voth, G. A.; Scuseria, G. E.; Frisch, M. J. Ab Initio Molecular Dynamics: Propagating the Density Matrix with Gaussian Orbitals. III. Comparison with Born-Oppenheimer Dynamics. *J. Chem. Phys.* **2002**, *117*, 8694–8704. https://doi.org/10.1063/1.1514582.
183. Bettens, R. P. A.; Collins, M. A. Learning to Interpolate Molecular Potential Energy Surfaces with Confidence: A Bayesian Approach. *J. Chem. Phys.* **1999**, *111*, 816–826. https://doi.org/10.1063/1.479368.
184. Behler, J. Representing Potential Energy Surfaces by High-Dimensional Neural Network Potentials. *J. Phys. Condens. Matter* **2014**, *26*, 183001. https://doi.org/10.1088/0953-8984/26/18/183001.
185. Manzhos, S.; Dawes, R.; Carrington, T. Neural Network-Based Approaches for Building High Dimensional and Quantum Dynamics-Friendly Potential Energy Surfaces. *Int. J. Quantum Chem.* **2015**, *115*, 1012–1020. https://doi.org/10.1002/qua.24795.
186. Yang, Y. N.; Zhang, S. H.; Ranasinghe, K. D.; Isayev, O.; Roitberg, A. E. Machine Learning of Reactive Potentials. *Annu. Rev. Phys. Chem.* **2024**, *75*, 371–395. https://doi.org/10.1146/annurev-physchem-062123-024417.
187. Habershon, S.; Manolopoulos, D. E.; Markland, T. E.; Miller, T. F. Ring-Polymer Molecular Dynamics: Quantum Effects in Chemical Dynamics from Classical Trajectories in an Extended Phase Space. In *Annual Review of Physical Chemistry*; Johnson, M. A., Martinez, T. J., Eds.; Annual Reviews: Palo Alto, CA, Vol. 64, 2013; pp 387–413.
188. Marx, D.; Tuckerman, M. E.; Martyna, G. J. Quantum Dynamics via Adiabatic Ab Initio Centroid Molecular Dynamics. *Comput. Phys. Commun.* **1999**, *118*, 166–184. https://doi.org/10.1016/s0010-4655(99)00208-8.
189. Shiga, M.; Nakayama, A. Ab Initio Path Integral Ring Polymer Molecular Dynamics: Vibrational Spectra of Molecules. *Chem. Phys. Lett.* **2008**, *451*, 175–181. https://doi.org/10.1016/j.cplett.2007.11.091.
190. Spura, T.; Elgabarty, H.; Kühne, T. D. "On-the-Fly" Coupled Cluster Path-Integral Molecular Dynamics: Impact of Nuclear Quantum Effects on the Protonated Water Dimer. *Phys. Chem. Chem. Phys.* **2015**, *17*, 14355–14359. https://doi.org/10.1039/c4cp05192k.
191. Buxton, S. J.; Habershon, S. Accelerated Path-Integral Simulations Using Ring-Polymer Interpolation. *J. Chem. Phys.* **2017**, *147*, 224107. https://doi.org/10.1063/1.5006465.
192. Karandashev, K.; Vanícek, J. A Combined On-the-Fly/Interpolation Procedure for Evaluating Energy Values Needed in Molecular Simulations. *J. Chem. Phys.* **2019**, *151*, 174116. https://doi.org/10.1063/1.5124469.
193. Zheng, J. J.; Frisch, M. J. Re-Integration with Anchor Points Algorithm for Ab Initio Molecular Dynamics. *J. Chem. Phys.* **2021**, *155*, 074106. https://doi.org/10.1063/5.0051079.

194. Jakowski, J.; Sumner, I.; Iyengar, S. S. Computational Improvements to Quantum Wave Packet Ab Initio Molecular Dynamics Using a Potential-Adapted, Time-Dependent Deterministic Sampling Technique. *J. Chem. Theory Comput*. **2006**, *2*, 1203–1219. https://doi.org/10.1021/ct600131g.
195. Iyengar, S. S.; Sumner, I.; Jakowski, J. Hydrogen Tunneling in an Enzyme Active Site: A Quantum Wavepacket Dynamical Perspective. *J. Phys. Chem. B* **2008**, *112*, 7601–7613. https://doi.org/10.1021/jp7103215.
196. Li, X. H.; Iyengar, S. S. Quantum Wavepacket Ab Initio Molecular Dynamics: Generalizations Using an Extended Lagrangian Treatment of Diabatic States Coupled through Multireference Electronic Structure. *J. Chem. Phys.* **2010**, *133*, 184105. https://doi.org/10.1063/1.3504167.
197. Li, J. J.; Li, X. H.; Iyengar, S. S. Vibrational Properties of Hydrogen-Bonded Systems Using the Multireference Generalization to the "On-the-Fly" Electronic Structure within Quantum Wavepacket Ab Initio Molecular Dynamics (QWAIMD). *J. Chem. Theory Comput*. **2014**, *10*, 2265–2280. https://doi.org/10.1021/ct5002347.
198. DeGregorio, N.; Iyengar, S. S. Efficient and Adaptive Methods for Computing Accurate Potential Surfaces for Quantum Nuclear Effects: Applications to Hydrogen-Transfer Reactions. *J. Chem. Theory Comput*. **2018**, *14*, 30–47. https://doi.org/10.1021/acs.jctc.7b00927.
199. Pavosevic, F.; Culpitt, T.; Hammes-Schiffer, S. Multicomponent Quantum Chemistry: Integrating Electronic and Nuclear Quantum Effects via the Nuclear-Electronic Orbital Method. *Chem. Rev.* **2020**, *120*, 4222–4253. https://doi.org/10.1021/acs.chemrev.9b00798.
200. Tao, Z.; Yu, Q.; Roy, S.; Hammes-Schiffer, S. Direct Dynamics with Nuclear-Electronic Orbital Density Functional Theory. *Acc. Chem. Res.* **2021**, *54*, 4131–4141. https://doi.org/10.1021/acs.accounts.1c00516.
201. Barbatti, M. Nonadiabatic Dynamics with Trajectory Surface Hopping Method. *Wiley Interdiscip. Rev. Comput. Mol. Sci.* **2011**, *1*, 620–633. https://doi.org/10.1002/wcms.64.
202. Curchod, B. F. E.; Rothlisberger, U.; Tavernelli, I. Trajectory-Based Nonadiabatic Dynamics with Time-Dependent Density Functional Theory. *ChemPhysChem* **2013**, *14*, 1314–1340. https://doi.org/10.1002/cphc.201200941.
203. Tapavicza, E.; Bellchambers, G. D.; Vincent, J. C.; Furche, F. Ab Initio Non-Adiabatic Molecular Dynamics. *Phys. Chem. Chem. Phys.* **2013**, *15*, 18336–18348. https://doi.org/10.1039/c3cp51514a.
204. Curchod, B. F. E.; Martínez, T. J. Ab Initio Nonadiabatic Quantum Molecular Dynamics. *Chem. Rev.* **2018**, *118*, 3305–3336. https://doi.org/10.1021/acs.chemrev.7b00423.
205. Crespo-Otero, R.; Barbatti, M. Recent Advances and Perspectives on Nonadiabatic Mixed Quantum-Classical Dynamics. *Chem. Rev.* **2018**, *118*, 7026–7068. https://doi.org/10.1021/acs.chemrev.7b00577.
206. Agostini, F.; Curchod, B. F. E. Different Flavors of Nonadiabatic Molecular Dynamics. *Wiley Interdiscip. Rev. Comput. Mol. Sci.* **2019**, *9*, e1417. https://doi.org/10.1002/wcms.1417.
207. Conti, I.; Cerullo, G.; Nenov, A.; Garavelli, M. Ultrafast Spectroscopy of Photoactive Molecular Systems from First Principles: Where we Stand Today and where we are Going. *J. Am. Chem. Soc.* **2020**, *142*, 16117–16139. https://doi.org/10.1021/jacs.0c04952.
208. Mai, S. B.; González, L. Molecular Photochemistry: Recent Developments in Theory. *Angew. Chem., Int. Ed.* **2020**, *59*, 16832–16846. https://doi.org/10.1002/anie.201916381.
209. Tully, J. C. Molecular-Dynamics with Electronic-Transitions. *J. Chem. Phys.* **1990**, *93*, 1061–1071. https://doi.org/10.1063/1.459170.
210. Jasper, A. W.; Stechmann, S. N.; Truhlar, D. G. Fewest-Switches with Time Uncertainty: A Modified Trajectory Surface-Hopping Algorithm with Better Accuracy for Classically Forbidden Electronic Transitions. *J. Chem. Phys.* **2002**, *116*, 5424–5431. https://doi.org/10.1063/1.1453404.
211. Zhu, C. Y.; Nangia, S.; Jasper, A. W.; Truhlar, D. G. Coherent Switching with Decay of Mixing: An Improved Treatment of Electronic Coherence for Non-Born-Oppenheimer Trajectories. *J. Chem. Phys.* **2004**, *121*, 7658–7670. https://doi.org/10.1063/1.1793991.
212. Li, X. S.; Tully, J. C.; Schlegel, H. B.; Frisch, M. J. Ab Initio Ehrenfest Dynamics. *J. Chem. Phys.* **2005**, *123*, 084106. https://doi.org/10.1063/1.2008258.
213. Suchan, J.; Liang, F.; Durden, A. S.; Levine, B. G. Prediction Challenge: First Principles Simulation of the Ultrafast Electron Diffraction Spectrum of Cyclobutanone. *J. Chem. Phys.* **2024**, *160*, 134310. https://doi.org/10.1063/5.0198333.
214. Makhov, D. V.; Symonds, C.; Fernandez-Alberti, S.; Shalashilin, D. V. Ab Initio Quantum Direct Dynamics Simulations of Ultrafast Photochemistry with Multiconfigurational Ehrenfest Approach. *Chem. Phys.* **2017**, *493*, 200–218. https://doi.org/10.1016/j.chemphys.2017.04.003.
215. Richings, G. W.; Polyak, I.; Spinlove, K. E.; Worth, G. A.; Burghardt, I.; Lasorne, B. Quantum Dynamics Simulations Using Gaussian Wavepackets: The vMCG Method. *Int. Rev. Phys. Chem.* **2015**, *34*, 269–308. https://doi.org/10.1080/0144235x.2015.1051354.